

Atomic worlds: current state and future of atom probe tomography in geoscience

D.W. Saxey^{*1}, D.E. Moser², S. Piazzolo^{3,4}, S.M. Reddy^{1,5}, J.W. Valley⁶

¹*Geoscience Atom Probe Facility, Advanced Resource Characterisation Facility, John de Laeter Centre, Curtin University, Perth, WA 6102, Australia.*

²*Department of Earth Sciences, University of Western Ontario, London, Canada N6A 5B7.*

³*Department of Earth and Planetary Science, Macquarie University, Sydney, NSW 2109, Australia.*

⁴*School of Earth and Environment, University of Leeds, Leeds LS2 9JT, UK.*

⁵*School of Earth and Planetary Sciences, Curtin University, Perth, WA 6102, Australia.*

⁶*Department of Geoscience, University of Wisconsin, Madison, WI 53706, USA.*

**Corresponding author: david.saxey@curtin.edu.au*

Abstract

Atom Probe Tomography (APT) is rapidly finding new applications within the geosciences. Historically connected with materials science and semiconductor device applications, recent years have seen APT established as a useful tool for nanoscale geochemistry, offering unique capabilities when compared with conventional geoanalytical techniques. The ability to characterize 3D nanoscale chemistry with isotopic sensitivity has uncovered intricate details of complex trace element distributions within a variety of minerals. Already these advances are having an impact on long-standing questions within geochronology, planetary science and other fields. Future developments are likely to bring significant expansion in this research space.

Keywords: atom probe tomography; three-dimensional atom probe (3DAP); atom probe microscopy; geochemistry; isotope geochemistry; geochronology;

Introduction

Earth's range of rock types represents different mixtures of over 5000 minerals, the diversity of which has grown over the past 4.4 billion years [1]. Each of these minerals has differing composition and/or crystal structure that reflects the conditions of formation and the

subsequent geological evolution that has modified them. Over several hundred years, geoscientists have developed a broad range of analytical techniques to characterize mineral compositions and structures, to shed light on the geological evolution of the planet. However, at a fundamental level, geological processes are governed by the mechanisms that control the nanoscale distribution and mobility of atoms within minerals and their boundaries. Nanoscale analytical techniques thereby underpin our ability to observe, measure and understand such mechanisms. At the sub-nanometer scale, transmission electron microscopy has commonly been used to investigate nanoscale processes in minerals [2–4]. However, this approach is limited to the compositional analysis of major elements and cannot identify individual atoms, or provide trace elements or isotopic compositions that are widely used by geochemists. In recent years, atom probe tomography (APT) has been increasingly applied to geological minerals to address this shortfall and to investigate a diverse and growing range of nanoscale features and processes. This contribution gives the authors' assessment of pioneering developments over the last few years, reviews the current state of APT in relation to geoscience applications, and forecasts the future developments and exciting possible applications in this rapidly growing field.

Atom Probe Tomography: A short overview

Atom probe tomography, often referred to alternatively as atom probe microscopy (APM), is unique among materials analysis techniques in its ability to provide three-dimensional chemical and isotopic information at near-atomic scales [5]. Such detailed analysis can be achieved over regions of interest of up to 100s of nm in size, carefully positioned at the apex of a needle-shaped specimen (Fig 1a). In its application to geological samples, which are commonly electrically insulating, the atom probe is usually operated in a 'pulsed-laser' mode, combining a very high electric field at the specimen tip with a short laser pulse focused in the same region [6]. Thermal energy from the laser pulse is sufficient to initiate field-evaporation of atoms from the specimen apex, ideally one atom at a time. The specimen is thereby slowly eroded away as the evaporated ions are accelerated from the tip and impact upon a position-sensitive detector (Fig. 1b). Data from the detector are used to infer the original 3-D location of

each atom within the sample, by applying a reverse-projection algorithm to the ion trajectories to generate a three-dimensional point-cloud, or 'atom map' (Fig. 1c). Importantly for geochemical studies, the detector arrival time can be used via time-of-flight mass spectrometry to determine the mass-to-charge ratio of each ion, which usually allows isotopes to be identified with confidence.

The mass-to-charge ratios are typically presented as a histogram, or 'mass spectrum' (Fig. 2). Interpretation of the data requires the association of intervals, or 'ranges', within the mass spectrum with particular ionic species [7], which may be elemental or molecular. Multiple charge states may also be present for a single species. No pre-selection of elements or isotopes is required as the entire spectrum is recorded for each laser pulse, and every atom may be considered to be ionized and detected with equal probability.

The ability to confidently interpret APT data requires both site-specific targeting from well-characterized locations and non-destructive, correlative imaging of the atom probe specimen. The workflow to identify critical locations commonly involves multiple techniques. In identifying regions of interest, geoscience atom probe studies have so far utilized SEM-based cathodoluminescence (CL) imaging [8–10], secondary ion mass spectrometry (SIMS) [9], laser ablation inductively coupled plasma mass spectrometry (LA-ICP-MS) [8], electron backscatter diffraction (EBSD) [10–12], x-ray fluorescence microscopy (XFM) [13], and backscatter electron (BSE) imaging [9,10,14]. Characterization of atom probe specimens by transmission Kikuchi diffraction (TKD) [15] in the SEM has been developed over recent years [16–18], and has been used to confirm lattice homogeneity of zircon and baddeleyite reference materials [19], and to identify subgrain boundaries and lattice distortions in zircon [11,12].

Geoscience applications of APT

Early work on geological materials was performed with voltage-pulsed atom probes, which require electrically conductive samples for efficient field-evaporation. This limited the quantity of data and the variety of materials that could be analysed [20,21]. The advent of

commercial laser atom probe systems in the mid-2000s opened the APT technique to non-conducting samples [22–25], including geological materials such as sulphides, carbonates and silicates. Combined with the ability to prepare site-specific samples using focused ion beam (FIB) techniques [26], this has resulted in a marked increase in the APT analysis of geological materials.

Over the last decade, a wide variety of mineral phases and multiphase samples have been analysed by APT. Although the majority of the Earth's accessible minerals are silicates, such as zircon (discussed below), much of the early use of atom probe samples for geomaterials is in the application to non-silicate phases such as oxides, sulphides, sulphates and metals. The earliest reported application to geomaterials is the analysis of a Ni-rich meteoritic alloy [21], with the first terrestrial study focusing on metamorphic magnetite [20].

Other mineral systems targeted by APT include triuranium octoxide (U_3O_8), an isotope standard, demonstrating the ability to distinguishing natural and anthropogenic sources of uranium at sub-micron scales [27]. Weber and co-workers [28] studied nanoscale structures in barite ($BaSO_4$), with implications for radium contamination. Analysis of a platinum group alloy [29] illustrated the applicability of APT in the study of metallic geomaterials, helping to decipher their origin.

Several researches have studied carbonate minerals via APT [30–33]. McMurray et al. [32], for example, investigated precipitation mechanisms of calcium carbonate in seawater. However, the application of APT to quantitative chemistry of carbonates still necessitates further development of the APT technique itself as carbonates, especially biominerals, are extremely beam sensitive, making it difficult to obtain reliable data [33].

In recent years, the application of APT on meteoritic materials has seen investigations of meteoritic nanodiamonds [34,35] and interfaces in kamacite-taenite, Fe-Ni alloys from the early solar system [36,37]. Several recent works have used APT to address planetary or proto-planetary processes [14,38–41]. For example, Daly et al. [14] analysed sub-micron refractory

metal nuggets to gain new insights into the spatial and temporal temperature and chemical variations in a protoplanetary disc.

The work to date on silicate minerals has focused on the application of atom probe tomography to understanding nanoscale trace element and isotopic variations in the common accessory mineral zircon (ZrSiO_4 , Fig. 3a,b). So far, the majority of studies have focused on understanding the mechanisms of Pb mobility and Pb loss, which have fundamental implications for the interpretation of U-Pb geochronological data.

The potential for APT to contribute to this field was first highlighted by Valley et al. [9,10], who analyzed a 4.4 billion year old zircon grain and showed that, despite Pb mobility and clustering at the nanoscale, the mineral remained a closed system for Pb at micron length scales and over geological timescales (Fig. 3a). Incompatible elements, including radiogenic Pb and rare earth elements have been shown to diffuse to amorphous domains created by radiation damage in zircons with complex histories [9,10]. Analysis of Pb isotope ratios in these 5-10nm clusters solve the Pb-mobility question at an atomic scale, confirm the age of the oldest known zircon from Earth, and represent the first application of nano-geochronology. Analysis of zircon that has lost Pb from its lattice has since shown that Pb distribution in zircon can be represented by isotopically-distinct Pb reservoirs, with nanoscale Pb-clusters being linked to dislocation loops formed during the annealing of U-induced radiation damage [8]. In these studies, the different Pb reservoirs yield different, but geologically-meaningful, age information that can be used to characterize different aspects of the mineral's geological evolution.

In deformed and deforming zircon, mineral defects are shown to control mobility of U and Pb [11] (Fig. 3b). Likewise, a study of zircon from the Stac Fada impactite showed mobility of coupled interstitial and substitutional trace elements linked to defect formation and migration over geologically-instantaneous timescales [12]. Similar approaches are starting to be applied to other U-bearing accessory minerals such as baddeleyite (ZrO_2) [41], where nano-clustering of trace elements, notably Fe, due to a meteorite impact shock wave has created

distinctive nanostructures (Fig. 3c). These serve as spatial proxies for crystal volumes that experienced Pb diffusion and record the crater age.

In summary, the studies have shown the importance of radiation damage and mineral defects in controlling element mobility, and that the recognition and quantification of different Pb isotopic ratios in nanoscale features has the potential to both advance our understanding of the controls on this mobility, and to yield new geochronological applications in a broad range of minerals.

The zircon studies are not only important to geochronology but also highlight fundamental mechanisms of processes that occur in any silicate; for example annealing-related elemental clustering and deformation-induced trace element mobility. Therefore, these studies are providing new ways to interpret trace element variations within and between grains of geologically important minerals such as olivine and pyroxene, with potential far-reaching implications for mantle flow and geodynamics.

Other work on silicate minerals includes early studies by several research groups on olivine [42–44], while Bachhav et al. were successful in targeting the chemical make-up of grain boundary structures in natural olivine and orthopyroxene [44].

Research with relevance to the resource industry includes the investigation of nanoscale gold clusters in arsenopyrite [13], which showed that the formation of nanoparticles of gold in arsenopyrite from the Obuasi gold mine of W. Africa was dependent upon crystal growth rates. This ability to characterize precious metal deportment at the nanoscale has fundamental implications for process mineralogy and the optimization of recovery efficiency.

Reference materials and standardisation

The novelty of APT as an analytical tool for geochemistry has prompted investigation of its performance and accuracy. In particular, zircon and badelleyite reference materials have been used to confirm chemical quantification and to optimise acquisition conditions for these minerals [19,45–48]. Conversely, APT has been employed to test the nanoscale homogeneity of existing geostandards [49]. Others have also reported comparisons between APT chemical and

isotopic compositions with those from standard materials or other well-characterised samples [9,27,29,33]. Initiatives have also been undertaken to develop standard approaches to the application of APT within the geosciences, including the proposed standardisation of data reporting [50].

Future Developments

Of central importance to geoscience applications of APT is the ability to correctly identify and quantify elemental and isotopic signatures of interest. Natural metals and minerals tend to have complex compositions in major, minor and trace elements and therefore yield mass spectra that have numerous peaks associated with both elemental species and a bewildering array of molecular species (Fig. 2). Although not unique to geological samples, such materials often yield molecular ions consisting of cation-anion complexes, in multiple charge states. Furthermore, the non-conductive nature of most geomaterials may result in significant ‘tails’ on mass spectrum peaks. As well as issues relating to peak identification, this complexity leads to interferences, which are difficult to resolve, and the dilution of low concentration trace elements over multiple, often immeasurable peaks. Consequently, many current challenges relate to optimization of the desired signal, and correct interpretation of these complex mass spectra. Other areas of development include improvements in the accuracy of the spatial three-dimensional reconstruction. In addition, the optimization of sample preparation will be crucial to open up APT to the general geoscience community, enabling routine, cost-effective, and well-constrained data production.

Several potential technical advances in APT hardware may bring significant improvements in the future. A modest increase in the mass resolving power, beyond the range of 1000 – 1200 typically attainable at present, could improve discrimination of overlapping mass peaks (Table 1). Improvements in detector efficiency [51] will lead to direct improvements in the quantification of nanoscale chemistry, as uncertainties are very often determined by fundamental limitations arising from the number of atom counts (counting statistics). Similarly, a reduction in detector dead-time could improve efficiency and quantification accuracy by ensuring that all ions are detected equally, even for closely-spaced isotopes. Continued

advances in spatial reconstruction accuracy will also play a role, though for the geosciences this aspect of APT data quality may not be as critical as in other applications [52–54]. However, accommodating large evaporation field differences associated with polyphase samples remains important [13,55], and advances in this area will be significant for geoscience studies.

A particularly exciting prospect for geological applications is the potential development of an energy-sensitive APT detector [56]. This would allow the mass spectra to be filtered for specific charge states, resulting in separation of mass peak overlaps and interferences [57], and a reduction in background noise (Fig 4). This would enable, for example, quantification of ^{208}Pb in zircon, as the $^{208}\text{Pb}^{++}$ and $^{28}\text{Si}_2^{16}\text{O}_3^+$ ions have different charge states. However, increased mass resolving power would still be required to separate ions having the same charge, such as the geologically important $^{40}\text{Ca}^{++}$ and $^{24}\text{Mg}^{16}\text{O}^{++}$ (Table 1).

Other potential hardware developments include the reduction of residual hydrogen gas in the ultra-high vacuum analysis chamber [58]. This could allow the quantification of water and other volatiles of importance within geological materials, including biologically mediated minerals, as well as reducing peak interferences due to hydride ion formation.

Advances are also likely to arise from improvements and innovations in methodology, particularly as APT is applied to a broader variety of mineral phases and their chemical variants. Progress has been made toward optimization of acquisition conditions and specimen preparation for some specific geological materials, such as zircon, baddeleyite, and magnetite [9,19,46,48,59,60], but many more sample types require similar attention and technique development. Suitable acquisition conditions may reduce detection limits for particular species, lower the background noise, simplify the mass spectrum, and eliminate peak overlaps by reducing complex molecular ion (e.g. hydride) formation [48]. Likewise, specimen preparation may be optimized to increase specimen yield, and also to reduce ‘thermal tails’ and improve the reproducibility of mass peak shapes. Such repeatability in mass peaks will be of critical importance in applying curve fitting techniques necessary to achieve robust background subtraction and mass peak deconvolution. As a wider variety of geological APT data becomes available, improvements in peak identification and the accurate quantification of peak

interferences, particularly hydrides, will provide valuable information required to completely separate and quantify isotopic concentrations.

Developments in correlative microscopy, particularly the use of combined physical and chemical characterization techniques such as TEM, TKD, and EBSD [61], along with Nano-Computed Tomography (CT), to identify and characterize regions of interest prior to APT analysis are also likely to play an important part in an advanced methodology for nanoscale geoscience. There is also potential for the integration of high spatial resolution compositional mapping tools such as sub-micron SIMS (nanoSIMS) [62,63] and SEM-based time-of-flight secondary ion mass spectrometry (TOF-SIMS) [64] to identify regions of interest at the sub-micrometre scale. In the geoscience field, characterization of needle-shaped specimens by transmission electron microscopy [65,66] has been undertaken only recently [37], but is likely to become a critical part of the work flow for robust interpretation of atom probe data. Further developments in specimen preparation will also enable a wider range of geological samples to be targeted, by providing robust methods for the analysis of nanoparticulate materials [34,67], or specimen preparation and coating methods to allow nano-porous or weakly-bonded materials to be analysed [67].

Applications: Examples and Outlook

Nanoscale geochemistry: from atomic-scale phenomena to large scale processes

The ability to analyse compositional information in 3D at close to atomic scales has the potential to revolutionise our understanding of the fundamental mechanisms that underpin many geological processes. Primary composition and compositional zoning of major and trace elements provides constraints on igneous [68], metamorphic [69] and sedimentary processes [70] in the Earth's crust and mantle [71], yet very few observations have been made at the nanoscale. Such observations have the potential to yield previously unobtainable information. Secondary processes that can alter elemental distributions in minerals, for example diffusion, will be modified by the presence and distribution of nanoscale defects and interfaces. Segregation of elements at the nanoscale has been shown to control the properties of non-geological materials [72], particularly their rheological behavior [73]. Yet there are currently

very few studies investigating the role of such features in geomaterials. The study of these features is clearly possible by APT and has the potential to change our understanding of mass transfer processes throughout geoscience, from biominerals to the formation of ore deposits. Such studies are not limited to Earth's crustal rocks. Volcanic activity may bring mantle samples to the surface, and meteorites represent accessible samples that formed on other bodies throughout the solar system's evolution. One potential challenge with such an approach is that the conditions by which nanoscale features form are often unknown in geological samples. One avenue to address this is in the analysis of minerals formed experimentally, where all extrinsic conditions are constrained. A combination of experimental and empirical approaches therefore seems to be a clear way forward. Such studies will be strengthened by simulations, utilizing molecular dynamics techniques to underpin observations with theoretical understanding [74].

Isotopic analysis: tracers and chronometers

Application of APT to radiogenic isotope geochemistry has been demonstrated using the U-Pb system [8–10]. And other radiogenic systems, such as Sm-Nd and Re-Os, also appear amenable to the technique, where concentrations permit [75]. Within this field, the atom probe is an ideal tool for determining the origin and history of geological materials from sub-micron isotopic signatures, which are often not resolvable using other techniques. Central to this application is the ability to accurately determine isotopic ratios from APT data. The highest accuracy is expected for single-element isotope ratios (e.g. $^{207}\text{Pb}/^{206}\text{Pb}$), which are aided by the absence of chemical-dependent effects on charge-state, molecular ion formation and mass peak shape [8–10,45]. For isotopic ratios between different elements (e.g. $^{206}\text{Pb}/^{238}\text{U}$) absolute quantification of each element is required with high accuracy. In these cases, optimization of acquisition conditions and developments in mass spectral data analysis will be essential for further advances.

Isotopic fractionation in stable isotope systems is also expected to be accessible to APT, though the necessary analytical precision is typically smaller than for radiogenic systems. As an indicator of potential applications, Table 2 compares a model uncertainty for fractionation data derived from APT measurements with the range of natural fractionation observed for each

element [76], assuming that isobaric interferences can be resolved. For many light element isotopes, which tend to exhibit significant fractionations due to their exchange mechanisms with fluids at low temperature, and the large relative mass difference between their isotopes, the sensitivity of APT over reasonable length scales is sufficient to detect meaningful levels of fractionation. The values are calculated for one million detected atoms and the uncertainty will reduce as more atoms are collected for a particular element. Depending on the atomic density of the sample and element composition, one million detected atoms corresponds to a 3-dimensional feature as small as 40 – 50nm. A significant challenge to development of stable isotope analysis via APT will be the avoidance or correction of mass interferences, particularly hydrides [9,34].

The aforementioned advances in mass spectrum peak shape determination and modelling would provide a step advance in the ability to quantify both chemical compositions and isotopic ratios by APT, and would open the possibility of analysing stable isotope systems at sub-micron scales. It is important to note that there is a fundamental limit to nanoscale chemical and isotopic measurements due to the granularity of atomic matter and the corresponding limitations imposed by Poissonian counting statistics that govern such sampling methods. However, APT is well-suited for approaching the limits of such measurements because of its relatively high ionization and detection efficiency (~80% in the CAMECA LEAP 5000X). Future technical advances, such as the reduction of detector dead-time, optimizations aimed at lowering background noise and peak tails, as well as increases in detector efficiency, will yield further incremental improvements in accuracy and sensitivity relevant to isotope geochemistry. Furthermore, a wide range of new experiments can be designed using synthetically enriched isotope ratios to investigate processes such as mineral-growth, unmixing, or diffusion at single-nanometer scale. Isotopic labels offer the advantage that different isotopes behave the same chemically yet can be distinguished by APT. If high concentrations of a trace isotope are added to an experiment, the contrast is identifiable at nanometer scales, allowing studies ranging from rate and process for diffusion and crystallization kinetics, to subcellular chemistry in microfossils.

Deformation and Defect Analysis

So far, the effect of deformation structures and dislocation movement on chemical variations at the nanometer scale has been shown only for zircon [11,12] and baddeleyite [40,41]. However, many other minerals may behave similarly. Importantly, the selectivity of the process of deformation induced elemental mobility will affect the elemental ratios, which are used for geothermobarometry (e.g. garnet, pyroxenes) and for determination of igneous and metasomatic history (e.g. olivine, [71]). Therefore, knowledge of deformation enhanced diffusion and elemental redistribution will be important across a variety of minerals, and not only those commonly used in geochronology (e.g. zircon, baddeleyite, apatite, titanite and rutile). In these cases, local changes to chemical composition significantly affect the geological interpretation of the rock from which the mineral stems.

Furthermore, it has been shown that incorporation of hydrogen in the crystal lattice has a marked effect on the rheology and slip system activation in geologically important minerals, such as olivine [77–79] and quartz [80]. For example, changes in hydrogen content in olivine will influence the seismic signal of deformed mantle rocks, which is used to infer mantle flow and large scale plate tectonic processes such as subduction zone behavior [81]. Consequently, in-depth understanding of the effect of deformation and deformation structures on hydrogen uptake and expulsion is of pivotal interest to the geoscience community.

Reaction interfaces and diffusion

The mechanisms by which reactions occur between individual mineral grains or between a mineral and a fluid (i.e. free water-rich fluid or melt) govern the progression of reactions, and with that the physiochemical behavior of geomaterials. The surface chemistry of the interface at the atomic scale plays a major role in these reactions [82], and APT is perfectly suited to investigate such interfaces, as evidenced by extensive applications within materials science [7,83–85]. APT is therefore likely to become an emerging technique for interface chemistry analysis of geomaterials.

Some related fields for which APT will be important include, leaching of contaminants from waste materials [86], weathering of surfaces (e.g. [82]), preservation of cultural heritage,

and metamorphic geology. In metamorphic geology, the rate of reaction progress is traditionally thought to depend on diffusion both within grains and at grain boundaries (e.g. [87]). A competing theory suggests that many reactions occur through fluid-mediated dissolution and precipitation [88], with much faster kinetics. With APT, this still unresolved question may be answered. In diffusion dominated reactions, the area right next to the interface of the reacting minerals should show a diffusion profile with elemental gradients; however, in the case of dissolution-precipitation reaction, a sharp, atomic-scale interface is expected [82,84,88].

Another application of APT is foreseen for diffusion studies [89–92], where the elemental diffusion profile at mineral interfaces is used to derive time-scales of volcanic-eruptions (e.g. [93,94]). For such studies, the spatial resolution offered by APT opens new avenues of diffusion profile modelling and verification against data from natural samples.

Standardisation of analytical procedure and data analysis

Finally, further studies are required to systematically investigate the influence of specimen preparation and the conditions of analysis on the accuracy of APT data across a variety of minerals. It is well established that APT analyses of oxides and other compound materials do not always yield accurate stoichiometric concentrations [60,95–100], and this often applies to the analysis of geological samples. Recent work has shown that chemical values derived from APT of zircon, at length scales of the specimen needle and below, are precise and reasonably accurate, though minor systematic discrepancies may arise depending on the analysis conditions [46,48]. A current effort from eight APT laboratories around the world is investigating these effects systematically using a reference material used in zircon geochronology [49], which has been shown to be chemically homogeneous at the nanometer scale. In the future, such rigorous evaluation of the accuracy of APT data will be necessary to better understand systematic compositional biases in other mineral types and their dependence on acquisition conditions and specimen geometry.

While reference materials, or standards, are widely used in ion- and electron-microprobe techniques, they are expected to be of limited use within APT. Although small

systematic errors are often present in the analysis [48], the technique does not lend itself to correction using standards, as the analysis conditions cannot be reliably replicated between the standard and the specimen of interest. In particular, the voltage applied to the specimen, the heating from the laser pulse and the shape of the specimen tip cannot be tightly controlled between acquisitions from two separate specimens.

Conclusions

The reconstruction of the nature and sequence of the processes that have created our planet and its resources is a major component of Earth and planetary science research, and is part of a discipline going back hundreds of years when ideas on the atomic makeup of minerals were just crystallizing. Atom probe tomography, in conjunction with other micro- and nano-analysis techniques, is thus opening up a broad new world of discovery. Even though a relatively small number of minerals has so far been explored, a diverse range of nano-features has already been revealed, corresponding to the formation of the solar system, early continents, giant craters, precious metals, and flowing deep crust in tectonic plates. Dozens of important rock-forming minerals from Earth and space remain to be analysed using current techniques, and studies of many diffusion phenomena in cool near-surface and deep, high-temperature environments have yet to be carried out. Promising developments in instrumentation to increase mass and spatial resolution, together with improved work flow through interfacing with reference and experimental samples, will amplify an already rapid pace of discovery with regard to atom probe tomography in geoscience.

Acknowledgements

The Geoscience Atom Probe at Curtin University is part of the Advanced Resource Characterisation Facility under the auspices of the National Resource Sciences Precinct—a collaboration between the Commonwealth Scientific and Industrial Research Organization, Curtin University, and the University of Western Australia—and is supported by the Science and Industry Endowment Fund (SIEF RI13-01). SP thanks the Australian Research Council for financial support (FT1101100070). DEM gratefully acknowledges research support through a Canadian NSERC-Discovery Grant. JWV is supported by the U.S. National Science Foundation

(EAR-1524336), the Department of Energy (DE-FG02- 93ER14389), and by NASA Award #NNA13AA94A, administered by the NASA Astrobiology Institute. The authors shared many fruitful discussions with Drs. David Larson, Tom Kelly, Dave Reinhard and other CAMECA-AMETEK scientists at the Madison, WI laboratory.

References

- [1] R.M. Hazen, D. Papineau, W. Bleeker, R.T. Downs, J.M. Ferry, T.J. McCoy, D.A. Sverjensky, H. Yang, *Am. Mineral.* 93 (2008) 1693–1720.
- [2] P. Buseck, J. Cowley, L. Eyring, *High-Resolution Transmission Electron Microscopy: And Associated Techniques*, Oxford University Press, 1989.
- [3] M.R. Lee, *Mineral. Mag.* 74 (2010) 1–27.
- [4] A.C. McLaren, *Transmission Electron Microscopy of Minerals and Rocks*, Cambridge University Press, 2005.
- [5] T.F. Kelly, D.J. Larson, *Annu. Rev. Mater. Res.* 42 (2012) 1–31.
- [6] D.J. Larson, T.J. Prosa, R.M. Ulfing, B.P. Geiser, T.F. Kelly, *Local Electrode Atom Probe Tomography*, Springer New York, New York, NY, 2013.
- [7] B. Gault, M.P. Moody, J.M. Cairney, S.P. Ringer, *Atom Probe Microscopy*, Springer New York, New York, NY, 2012.
- [8] E.M. Peterman, S.M. Reddy, D.W. Saxey, D.R. Snoeyenbos, W.D.A. Rickard, D. Fougereuse, A.R.C. Kylander-Clark, *Sci. Adv.* 2 (2016) e1601318.
- [9] J.W. Valley, D.A. Reinhard, A.J. Cavosie, T. Ushikubo, D.F. Lawrence, D.J. Larson, T.F. Kelly, D.R. Snoeyenbos, A. Strickland, *Am. Mineral.* 100 (2015) 1355–1377.
- [10] J.W. Valley, A.J. Cavosie, T. Ushikubo, D.A. Reinhard, D.F. Lawrence, D.J. Larson, P.H. Clifton, T.F. Kelly, S.A. Wilde, D.E. Moser, M.J. Spicuzza, *Nat. Geosci.* 7 (2014) 219–223.
- [11] S. Piazzolo, A. La Fontaine, P. Trimby, S. Harley, L. Yang, R. Armstrong, J.M. Cairney, *Nat. Commun.* 7 (2016) 10490.
- [12] S.M. Reddy, A. van Riessen, D.W. Saxey, T.E. Johnson, W.D.A. Rickard, D. Fougereuse, S. Fischer, T.J. Prosa, K.P. Rice, D.A. Reinhard, Y. Chen, D. Olson, *Geochim. Cosmochim. Acta* 195 (2016) 158–170.
- [13] D. Fougereuse, S.M. Reddy, D.W. Saxey, W.D.A. Rickard, A. van Riessen, S. Micklethwaite, *Am. Mineral.* 101 (2016) 1916–1919.
- [14] L. Daly, P.A. Bland, D.W. Saxey, S.M. Reddy, D. Fougereuse, W.D.A. Rickard, L.V. Forman, *Geology* 45 (2017) 847–850.
- [15] P.W. Trimby, *Ultramicroscopy* 120 (2012) 16–24.
- [16] K. Babinsky, R. De Kloe, H. Clemens, S. Primig, *Ultramicroscopy* 144 (2014) 9–18.
- [17] A.J. Breen, K. Babinsky, A.C. Day, K. Eder, C.J. Oakman, P.W. Trimby, S. Primig, J.M. Cairney, S.P. Ringer, *Microsc. Microanal.* (2017) 1–12.

- [18] K.P. Rice, Y. Chen, T.J. Prosa, D.J. Larson, *Microsc. Microanal.* 22 (2016) 583–588.
- [19] D.A. Reinhard, D.E. Moser, I. Martin, K.P. Rice, Y. Chen, D. Olson, D.F. Lawrence, T.J. Prosa, D.J. Larson, in: D.E. Moser, F. Corfu, J.R. Darling, S.M. Reddy, K.T. Tait (Eds.), *Microstruct. Geochronol.*, AGU/Wiley Publishing, 2017.
- [20] K.R. Kuhlman, R.L. Martens, T.F. Kelly, N.D. Evans, M.K. Miller, *Ultramicroscopy* 89 (2001) 169–176.
- [21] M.K. Miller, K.F. Russell, *Surf. Sci.* 266 (1992) 441–445.
- [22] J.H. Bunton, J.D. Olson, D.R. Lenz, T.F. Kelly, *Microsc. Microanal.* 13 (2007) 418–427.
- [23] B. Deconihout, F. Vurpillot, B. Gault, G. Da Costa, M. Bouet, A. Bostel, D. Blavette, A. Hideur, G. Martel, M. Brunel, *Surf. Interface Anal.* 39 (2007) 278–282.
- [24] B. Gault, F. Vurpillot, A. Vella, M. Gilbert, A. Menand, D. Blavette, B. Deconihout, *Rev. Sci. Instrum.* 77 (2006) 043705.
- [25] K. Hono, T. Ohkubo, Y.M. Chen, M. Kodzuka, K. Oh-ishi, H. Sepehri-Amin, F. Li, T. Kinno, S. Tomiya, Y. Kanitani, *Ultramicroscopy* 111 (2011) 576–583.
- [26] M.K. Miller, K.F. Russell, K. Thompson, R. Alvis, D.J. Larson, *Microsc. Microanal.* 13 (2007) 428–436.
- [27] A.J. Fahey, D.E. Perea, J. Bartrand, B.W. Arey, S. Thevuthasan, *J. Environ. Radioact.* 153 (2016) 206–213.
- [28] J. Weber, J. Barthel, F. Brandt, M. Klinkenberg, U. Breuer, M. Kruth, D. Bosbach, *Chem. Geol.* 424 (2016) 51–59.
- [29] S.W. Parman, D.R. Diercks, B.P. Gorman, R.F. Cooper, *Am. Mineral.* 100 (2015) 852–860.
- [30] O. Branson, E.A. Bonnin, D.E. Perea, H.J. Spero, Z. Zhu, M. Winters, B. Hönisch, A.D. Russell, J.S. Fehrenbacher, A.C. Gagnon, *Proc. Natl. Acad. Sci.* (2016) 201522864.
- [31] A.R. Felmy, O. Qafoku, B.W. Arey, L. Kovarik, J. Liu, D. Perea, E.S. Ilton, *Chem. Geol.* 395 (2015) 119–125.
- [32] S. McMurray, B. Gorman, D. Diercks, *Microsc. Microanal.* 17 (2011) 758–759.
- [33] A. Pérez-Huerta, F. Laiginhas, D.A. Reinhard, T.J. Prosa, R.L. Martens, *Micron* 80 (2016) 83–89.
- [34] P.R. Heck, F.J. Stadermann, D. Isheim, O. Auciello, T.L. Daulton, A.M. Davis, J.W. Elam, C. Floss, J. Hiller, D.J. Larson, J.B. Lewis, A. Mane, M.J. Pellin, M.R. Savina, D.N. Seidman, T. Stephan, *Meteorit. Planet. Sci.* 49 (2014) 453–467.
- [35] J.B. Lewis, D. Isheim, C. Floss, D.N. Seidman, *Ultramicroscopy* 159 (2015) 248–254.
- [36] S.S. Rout, P.R. Heck, D. Isheim, T. Stephan, A.M. Davis, D.N. Seidman, *Microsc. Microanal.* 21 (2015) 1313–1314.
- [37] S.S. Rout, P.R. Heck, D. Isheim, T. Stephan, N.J. Zaluzec, D.J. Miller, A.M. Davis, D.N. Seidman, *Meteorit. Planet. Sci.* (2017).

- [38] P. Gopon, M.J. Spicuzza, T.F. Kelly, D. Reinhard, T.J. Prosa, J. Fournelle, *Meteorit. Planet. Sci.* 52 (2017) 1941–1962.
- [39] B.P. Gorman, D.R. Diercks, S. Parman, R. Cooper, *Microsc. Microanal.* 21 (2015) 1311–1312.
- [40] L.F. White, J.R. Darling, D.E. Moser, D.A. Reinhard, J. Dunlop, D.J. Larson, in: D.E. Moser, F. Corfu, J.R. Darling, S.M. Reddy, K.T. Tait (Eds.), *Microstruct. Geochronol.*, AGU/Wiley Publishing, 2017.
- [41] L.F. White, J.R. Darling, D.E. Moser, D.A. Reinhard, T.J. Prosa, D. Bullen, D. Olson, D.J. Larson, D. Lawrence, I. Martin, *Nat. Commun.* 8 (2017) 15597.
- [42] B.W. Arey, D. Perera, L. Kovarik, O. Qafoku, A. Felmy, B. Gorman, *Microsc. Microanal.* 18 (2012) 658–659.
- [43] B.W. Arey, D.E. Perea, L. Kovarik, R.J. Colby, J. Liu, O. Qafoku, A.R. Felmy, *Microsc. Microanal.* 20 (2014) 998–999.
- [44] M. Bachhav, Y. Dong, P. Skemer, E.A. Marquis, *Microsc. Microanal.* 21 (2015) 1315–1316.
- [45] T. Blum, D.A. Reinhard, Y. Chen, T.J. Prosa, J.W. Valley, in: D.E. Moser, F. Corfu, J.R. Darling, S.M. Reddy, K.T. Tait (Eds.), *Microstruct. Geochronol.*, AGU/Wiley Publishing, 2017.
- [46] A. La Fontaine, S. Piazzolo, P. Trimby, L. Yang, J.M. Cairney, *Microsc. Microanal.* (2017) 1–10.
- [47] D.A. Reinhard, D.E. Moser, I.R. Barker, D. Olson, I. Martin, K.P. Rice, Y. Chen, D. Lawrence, T.J. Prosa, D.J. Larson, *Microsc. Microanal.* 21 (2015) 851–852.
- [48] D.W. Saxey, S.M. Reddy, D. Fougereuse, W.D.A. Rickard, in: D.E. Moser, F. Corfu, J.R. Darling, S.M. Reddy, K.T. Tait (Eds.), *Microstruct. Geochronol.*, AGU/Wiley Publishing, 2017.
- [49] S. Piazzolo, E. Belousova, A. La Fontaine, C. Corcoran, J.M. Cairney, *Chem. Geol.* 456 (2017) 10–18.
- [50] T. Blum, J. Darling, T.F. Kelly, D.J. Larson, D.E. Moser, A. Perez-Huerta, T.J. Prosa, S. Reddy, D.A. Reinhard, D. Saxey, R. Ulfig, J.W. Valley, in: D.E. Moser, F. Corfu, J.R. Darling, S.M. Reddy, K.T. Tait (Eds.), *Microstruct. Geochronol.*, AGU/Wiley Publishing, 2017.
- [51] T.F. Kelly, *Microsc. Microanal.* 23 (2017) 34–45.
- [52] T.F. Kelly, D.J. Larson, K. Thompson, R.L. Alvis, J.H. Bunton, J.D. Olson, B.P. Gorman, *Annu. Rev. Mater. Res.* 37 (2007) 681–727.
- [53] D.J. Larson, B. Gault, B.P. Geiser, F. De Geuser, F. Vurpillot, *Curr. Opin. Solid State Mater. Sci.* 17 (2013) 236–247.
- [54] F. Vurpillot, N. Rolland, R. Estivill, S. Duguay, D. Blavette, *Semicond. Sci. Technol.* 31 (2016) 074002.
- [55] N. Rolland, D.J. Larson, B.P. Geiser, S. Duguay, F. Vurpillot, D. Blavette, *Ultramicroscopy* 159 (2015) 195–201.

- [56] T.F. Kelly, *Microsc. Microanal.* 17 (2011) 1–14.
- [57] S.R. Broderick, A. Bryden, S.K. Suram, K. Rajan, *Ultramicroscopy* 132 (2013) 121–128.
- [58] Y. Ishikawa, V. Nemanič, *Vacuum* 69 (2003) 501–512.
- [59] L.M. Gordon, D. Joester, *Nature* 469 (2011) 194–197.
- [60] D.K. Schreiber, A.N. Chiaramonti, L.M. Gordon, K. Kruska, *Appl. Phys. Lett.* 105 (2014) 244106.
- [61] S.M. Reddy, D.W. Saxey, W.D.A. Rickard, D. Fougerouse, A. van Riessen, in: *Conf. Proc. EMAS 2017 IUMAS-7, Konstanz, Germany, 2017*, pp. 150–158.
- [62] D.K. Schreiber, M.J. Olszta, D.W. Saxey, K. Kruska, K.L. Moore, S. Lozano-Perez, S.M. Bruemmer, *Microsc. Microanal.* 19 (2013) 676–687.
- [63] J.B. Seol, N.S. Lim, B.H. Lee, L. Renaud, C.G. Park, *Met. Mater. Int.* 17 (2011) 413–416.
- [64] W.D.A. Rickard, S.M. Reddy, D.W. Saxey, D. Fourgerouse, A. van Riessen, in: *Proc. Microsc. Microanal. 2016, Microscopy Society of America, Columbus, Ohio, 2016*, pp. 684–685.
- [65] M. Herbig, *Scr. Mater.* (2017).
- [66] W. Lefebvre-Ulrikson, in: *W. Lefebvre, F. Vurpillot, X. Sauvage (Eds.), At. Probe Tomogr. Put Theory Pract., 1st ed., Academic Press, 2016*.
- [67] P. Felfer, T. Li, K. Eder, H. Galinski, A.P. Magyar, D.C. Bell, G.D.W. Smith, N. Kruse, S.P. Ringer, J.M. Cairney, *Ultramicroscopy* 159 (2015) 413–419.
- [68] C. Ginibre, G. Wörner, A. Kronz, *Elements* 3 (2007) 261–266.
- [69] M.J. Kohn, S.L. Corrie, *Earth Planet. Sci. Lett.* 311 (2011) 136–143.
- [70] T. Götte, T. Pettke, K. Ramseyer, M. Koch-Muller, J. Mullis, *Am. Mineral.* 96 (2011) 802–813.
- [71] S.F. Foley, D. Prelevic, T. Rehfeldt, D.E. Jacob, *Earth Planet. Sci. Lett.* 363 (2013) 181–191.
- [72] E.A. Marquis, M. Bachhav, Y. Chen, Y. Dong, L.M. Gordon, A. McFarland, *Curr. Opin. Solid State Mater. Sci.* 17 (2013) 217–223.
- [73] S. Floreen, J. Westbrook, *Acta Metall.* 17 (1969) 1175–1181.
- [74] R. Skelton, A.M. Walker, *Phys. Chem. Miner.* 42 (2015) 677–691.
- [75] L. Daly, P.A. Bland, L.V. Forman, D.W. Saxey, S.M. Reddy, W.D.A. Rickard, D. Fougerouse, S. Tessalina, A.L. Fontaine, L. Yang, P.W. Trimby, J. Cairney, S.P. Ringer, B.F. Schaefer, in: *80th Annu. Meet. Meteorit. Soc., 2017*.
- [76] J. Hoefs, *Stable Isotope Geochemistry*, Springer International Publishing, Cham, 2015.
- [77] S.-I. Karato, M.S. Paterson, J.D. FitzGerald, *J. Geophys. Res. Solid Earth* 91 (1986) 8151–8176.
- [78] I. Katayama, H. Jung, S. Karato, *Geology* 32 (2004) 1045–1048.
- [79] J. Korenaga, S.-I. Karato, *J. Geophys. Res.* 113 (2008) B02403.
- [80] A.K. Kronenberg, J. Tullis, *J. Geophys. Res. Solid Earth* 89 (1984) 4281–4297.

- [81] I. Katayama, S. Karato, *Phys. Earth Planet. Inter.* 157 (2006) 33–45.
- [82] R. Hellmann, R. Wirth, D. Daval, J.-P. Barnes, J.-M. Penisson, D. Tisserand, T. Epicier, B. Florin, R.L. Hervig, *Chem. Geol.* 294–295 (2012) 203–216.
- [83] A. Devaraj, D.E. Perea, J. Liu, L.M. Gordon, T.J. Prosa, P. Parikh, D.R. Diercks, S. Meher, R.P. Kolli, Y.S. Meng, S. Thevuthasan, *Int. Mater. Rev.* (2017) 1–34.
- [84] R. Hellmann, S. Cotte, E. Cadel, S. Malladi, L.S. Karlsson, S. Lozano-Perez, M. Cabié, A. Seyeux, *Nat. Mater.* 14 (2015) 307–311.
- [85] M.K. Miller, *J. Mater. Sci.* 41 (2006) 7808–7813.
- [86] C.S. Kirby, J.D. Rimstidt, *Environ. Sci. Technol.* 28 (1994) 443–451.
- [87] R.H. Vernon, G.L. Clarke, *Principles of Metamorphic Petrology*, Cambridge University Press, 2008.
- [88] A. Putnis, *Rev. Mineral. Geochem.* 70 (2009) 87–124.
- [89] O. Cojocar-Mirédin, C. Perrin-Pellegrino, D. Mangelinck, D. Blavette, *Microelectron. Eng.* 87 (2010) 271–273.
- [90] D. Mangelinck, K. Houmada, A. Portavoce, C. Perrin, R. Daineche, M. Descoins, D.J. Larson, P.H. Clifton, *Scr. Mater.* 62 (2010) 568–571.
- [91] S. Park, W. Jung, C. Park, *Met. Mater. Int.* 19 (2013) 1117–1121.
- [92] G. Schmitz, C.-B. Ene, C. Nowak, *Acta Mater.* 57 (2009) 2673–2683.
- [93] G.N. Kilgour, K.E. Saunders, J.D. Blundy, K.V. Cashman, B.J. Scott, C.A. Miller, *J. Volcanol. Geotherm. Res.* 288 (2014) 62–75.
- [94] D.J. Morgan, S. Blake, N.W. Rogers, B. DeVivo, G. Rolandi, R. Macdonald, C.J. Hawkesworth, *Earth Planet. Sci. Lett.* 222 (2004) 933–946.
- [95] A. Devaraj, R. Colby, W.P. Hess, D.E. Perea, S. Thevuthasan, *J. Phys. Chem. Lett.* 4 (2013) 993–998.
- [96] M. Karahka, H.J. Kreuzer, *Ultramicroscopy* 132 (2013) 54–59.
- [97] N. Amirifar, R. Lardé, E. Talbot, P. Pareige, L. Rigutti, L. Mancini, J. Houard, C. Castro, V. Sallet, E. Zehani, others, *J. Appl. Phys.* 118 (2015) 215703.
- [98] J.R. Riley, R.A. Bernal, Q. Li, H.D. Espinosa, G.T. Wang, L.J. Lauhon, *ACS Nano* 6 (2012) 3898–3906.
- [99] D.R. Diercks, B.P. Gorman, R. Kirchhofer, N. Sanford, K. Bertness, M. Brubaker, *J. Appl. Phys.* 114 (2013) 184903.
- [100] L. Mancini, N. Amirifar, D. Shinde, I. Blum, M. Gilbert, A. Vella, F. Vurpillot, W. Lefebvre, R. Lardé, E. Talbot, P. Pareige, X. Portier, A. Ziani, C. Davesne, C. Durand, J. Eymery, R. Butté, J.-F. Carlin, N. Grandjean, L. Rigutti, *J. Phys. Chem. C* 118 (2014) 24136–24151.

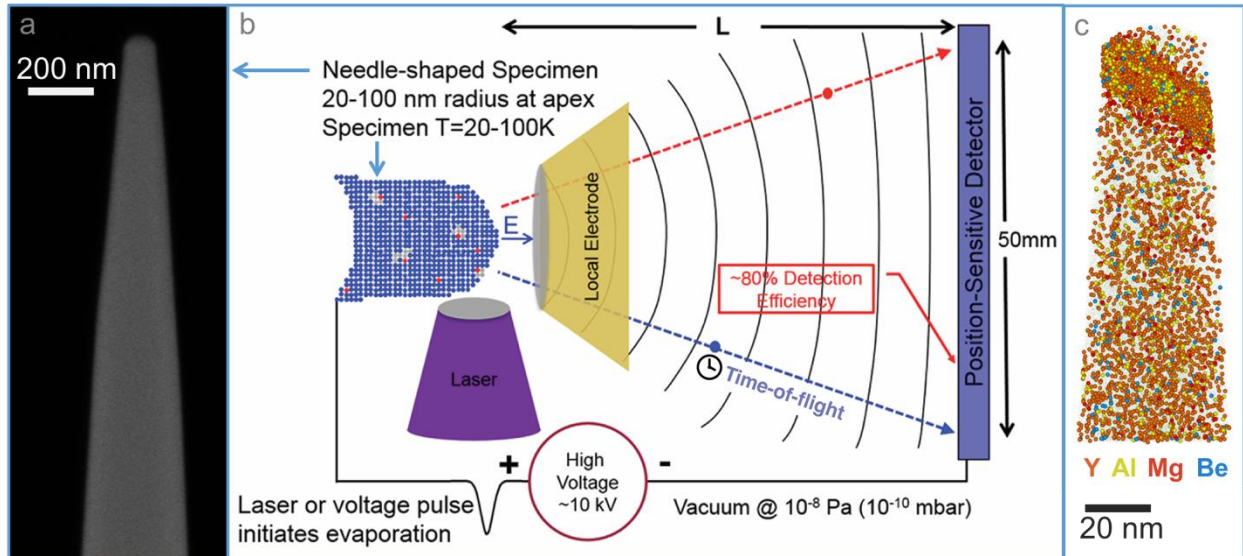


Figure 1: a) Scanning electron microscope image of an APT specimen needle. b) Schematic view of the atom probe microscope from Valley et al. [9]. The laser pulse incident on the specimen apex initiates field-evaporation of ions from the surface. Ions are projected by the strong electrostatic field on to the position-sensitive detector, creating a highly magnified 'image' of the specimen surface. Measurement of the ion flight times, from laser pulse to detector impact, allows the ion identities to be determined by time-of-flight mass spectrometry. c) The detector data can be used to reconstruct the original three-dimensional location of each detected atom within the specimen. The atom map here shows the distribution of trace elements within a sample of shocked zircon [12].

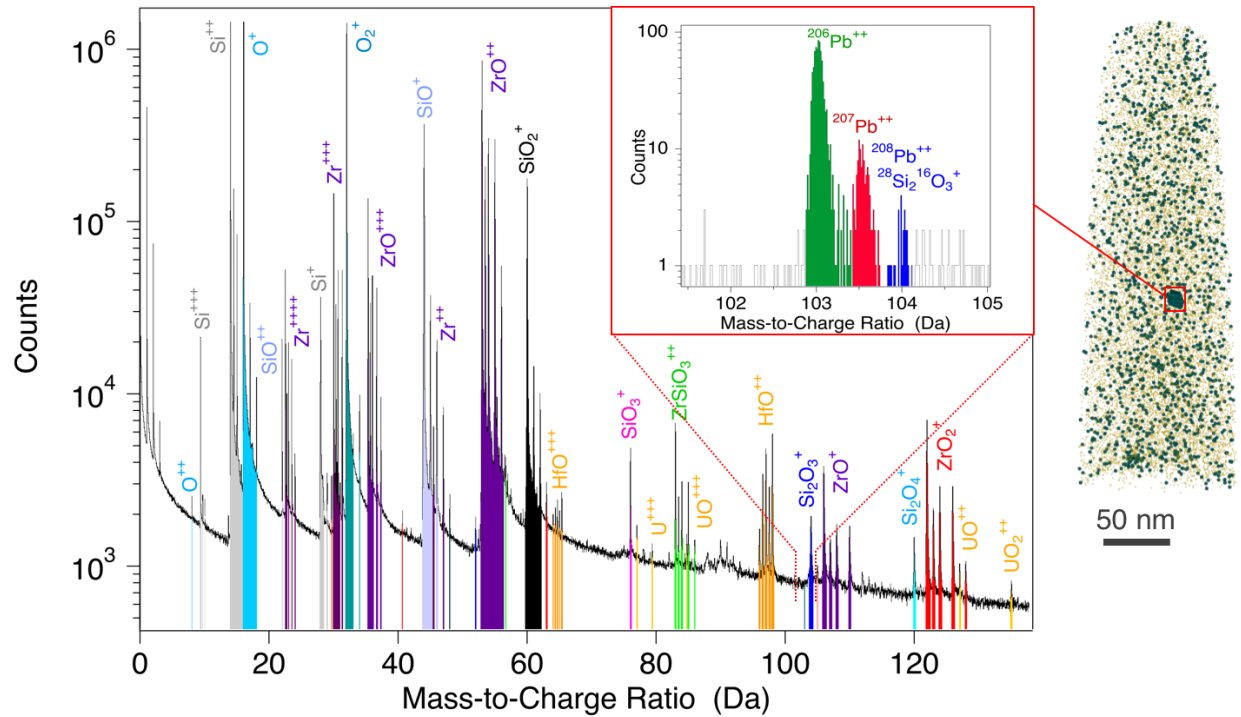


Figure 2: An APT mass spectrum obtained from a zircon sample, showing the ranges (coloured bands) used to identify each atomic or molecular ion species. The atom map (right side) shows the distribution of Pb atoms within the grain. Selecting only the atoms in close proximity to a ~ 10 nm Pb-rich cluster allows the Pb isotopes to be clearly identified in the reduced mass spectrum (inset). From Peterman et al. [8].

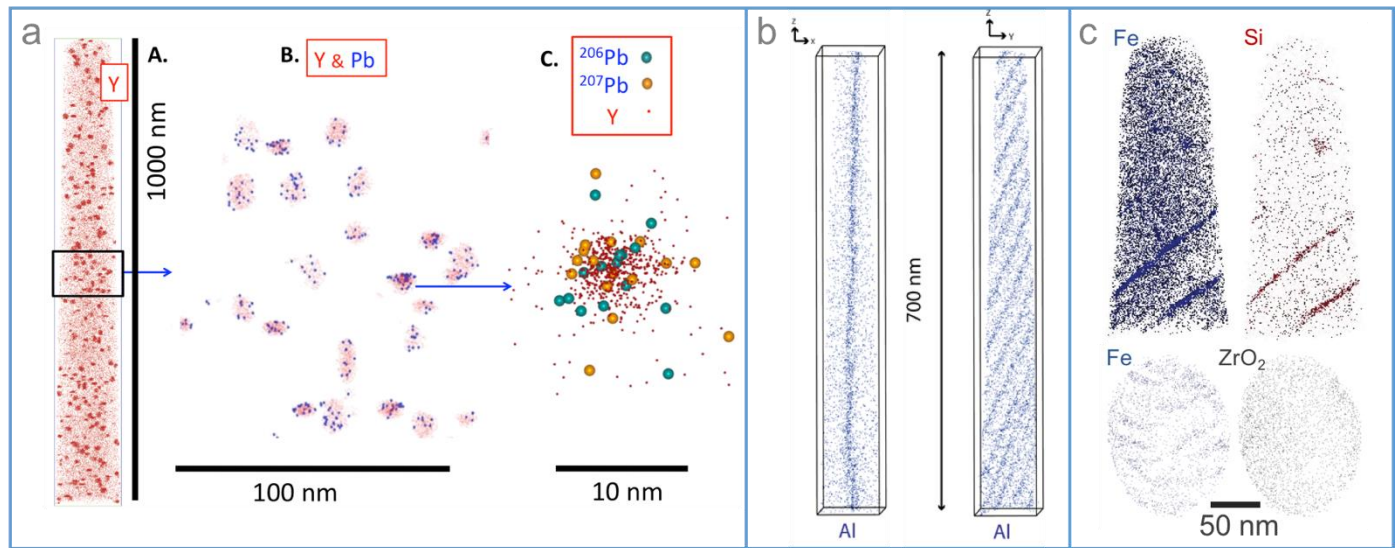


Figure 3:

a) APT of zircons ($ZrSiO_4$). A: Full specimen 3D atom map ($\sim 1000 \times 100$ nm) from a 4.4 billion year old zircon showing the distribution of Y atoms. Darker domains are clusters of 100's of atoms. B: Clusters from A are isolated and enlarged, showing atoms of Y (orange) and Pb (blue) co-localized in clusters. C: Single cluster from B: Y (orange), ^{206}Pb (green), ^{207}Pb (yellow). Y and rare earth elements are concentrated by a factor of 60 in clusters, which have average diameters of 5-10 nm and closest-neighbor spacing averaging 25 nm. The ratios of $^{207}Pb/^{206}Pb$ show that Pb is radiogenic and that clusters formed ca 1 billion years later than the zircon. Clusters are interpreted to form by diffusion of Pb and rare earth elements to amorphous domains formed by alpha-recoil of daughter atoms on emission of α -particles. These results confirm the age of the oldest known solid material from Earth and are interpreted to indicate that conditions habitable for life existed on Earth over 800 million years before the earliest known microfossils. From Valley et al. [9,10].

b) Distribution of aluminium atoms on a low angle grain boundary in a 2.5 billion year old deformed zircon grain. Note the 90 degrees rotation between the two atom maps. The Al atoms decorate a regularly spaced array of dislocation cores that form the boundary. The authors interpret that this decoration is a consequence of trace element attraction and accumulation during dislocation movement. Consequently, crystal plastic deformation can significantly change the local elemental make up of a mineral. From Piazzolo et al. [11].

c) APT atom maps from a 2.5 billion year old baddeleyite (monoclinic zirconia (ZrO_2)) grain from the edge of the 1.85 billion year old Sudbury meteorite-impact structure, Canada. The data illustrate the clustering and re-distribution of trace elements such as Fe and Si to form planar features attributed to the shock wave and deformation that accompanied crater and massive Cu-Ni ore deposit formation. Note the crescent shaped nano-structures apparent in plan views of the planar sub-volumes. From White et al. [41].

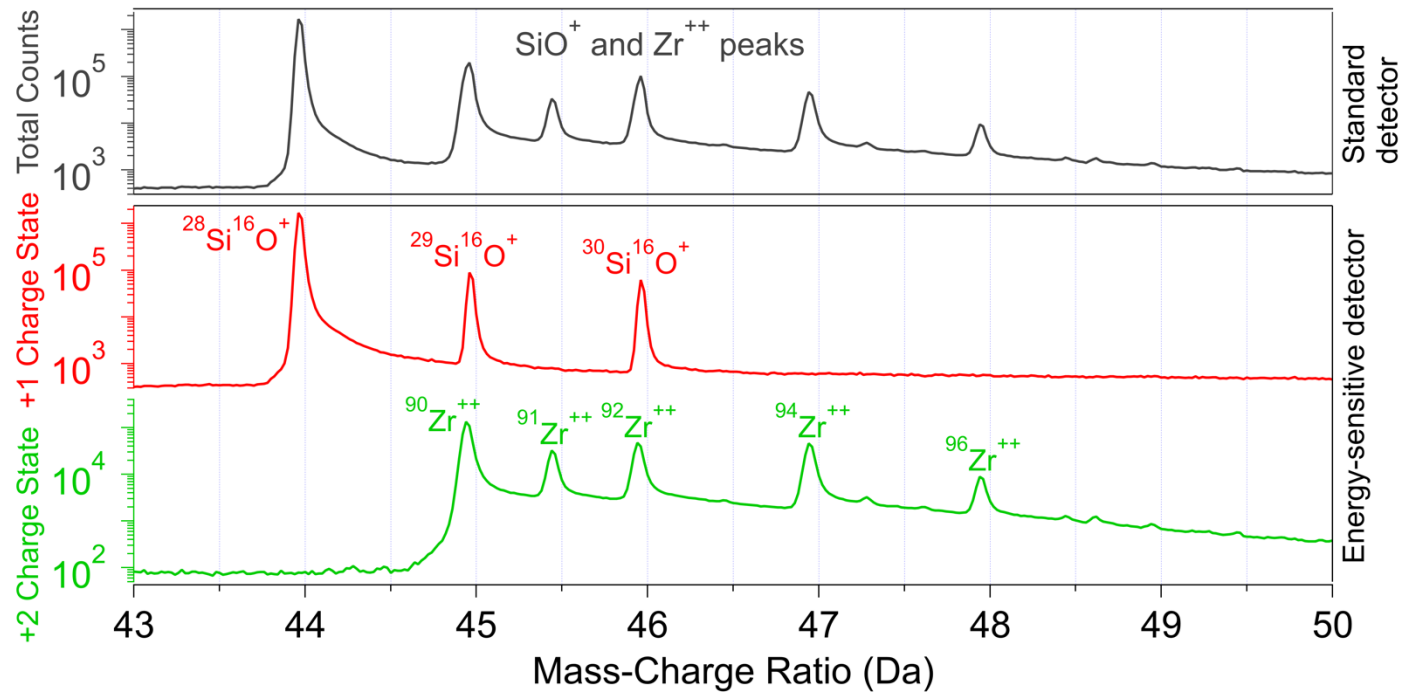


Figure 4: Indicative spectra showing the expected peak decomposition achievable with an energy-sensitive detector having sufficient resolution to separate +1 and +2 charge states (i.e. a factor of 2 in energy). Data shows part of a zircon mass spectrum.

Ion peak interferences		m/Δm
$^{51}\text{V}^+$	$^{27}\text{Al}_2\text{O}_3^{++}$	1702
$^{48}\text{TiO}^{++}$	$^{16}\text{O}_2^+$	1740
$^{208}\text{Pb}^{++}$	$^{28}\text{Si}_2\text{O}_3^+$	2090
$^{40}\text{Ca}^{++}$	$^{24}\text{MgO}^{++}$	2300
$^{13}\text{C}^+$	$^{12}\text{CH}^+$	2910

Table 1: The mass resolving power ($m/\Delta m$) required to separate various mass peak interferences.

Element, Stable isotopes	Minor isotope abundance (%)	Estimated APT measurement uncertainty in isotope ratio (1 std dev ‰)	Approximate range of ratios in terrestrial isotope geochemistry (‰)
H (2/1)	0.016%	79	400
Li (7/6)	7.59%	3.6	50
B (11/10)	19.90%	2.2	40
C (13/12)	1.07%	9.7	30
N (15/14)	0.36%	16.6	20
O (18/16)	0.21%	22.1	100
S (34/32)	4.20%	4.9	100

Table 2: Model uncertainties (1 SD) for stable isotope ratios, as determined by APT, are compared with the approximate range of isotope ratios that are observed in natural samples [76]. The APT uncertainty estimate is derived from the counting statistics of the least abundant isotope in the ratio, based on the detection of one million atoms across all isotopes of each element, and assuming no unresolved interferences.